Thermalization of the Lipkin-Meshkov-Glick model in blackbody radiation

T. Macrì,[1] M. Ostilli,[2] and C. Presilla[3,4]

[1]*Departamento de Física Téorica e Experimental and International Institute of Physics, Universidade Federal do Rio Grande do Norte, Natal-RN, Brazil*
[2]*Departamento de Física Téorica e Experimental, Universidade Federal do Rio Grande do Norte, Natal-RN, Brazil*
[3]*Dipartimento di Fisica, Sapienza Università di Roma, Piazzale A. Moro 2, Roma 00185, Italy*
[4]*Istituto Nazionale di Fisica Nucleare, Sezione di Roma 1, Roma 00185, Italy*

In a recent work, we have derived simple Lindblad-based equations for the thermalization of systems in contact with a thermal reservoir. Here, we apply these equations to the Lipkin-Meshkov-Glick model in contact with blackbody radiation and analyze the dipole matrix elements involved in the thermalization process. We find that the thermalization can be complete only if the density is sufficiently high, while, in the limit of low density, the system thermalizes partially, namely, within the Hilbert subspaces where the total spin has a fixed value. In this regime, and in the isotropic case, we evaluate the characteristic thermalization time analytically, and show that it diverges with the system size in correspondence with the critical points and inside the ferromagnetic region. Quite interestingly, at zero temperature the thermalization time diverges only quadratically with the system size, whereas quantum adiabatic algorithms, aimed at finding the ground state of the same system, imply a cubic divergence of the required adiabatic time.

I. INTRODUCTION

The main difference between open and isolated systems is the lack of conservation laws in the former, the most common one being the energy conservation. For open quantum systems [1–3], another peculiar but less uniquely defined quantity, quantum coherence, is being lost. In more formal terms, if the system, when isolated, is governed by some time-independent Hamiltonian $\boldsymbol{H}$, and if $\boldsymbol{O}_1, \ldots, \boldsymbol{O}_q$ are a set of q-independent operators that commute with $\boldsymbol{H}$, and commute with each other, the quantum-mechanical averages of these operators, including $\boldsymbol{H}$, provide a set of $q + 1$ constants of motion. If instead the system interacts with some environment, in general, none of these operators is a constant of motion. Nevertheless, if the system-environment interaction can be reduced to one of the operators $\boldsymbol{O}_1, \ldots, \boldsymbol{O}_q$, say $\boldsymbol{O}_1$, then, even if the system loses both energy and quantum coherence, $\boldsymbol{O}_1$ remains conserved during what we can call a partial thermalization process. This is what happens in the Lipkin-Meshkov-Glick (LMG) model [4] when put in contact with a thermal reservoir constituted by blackbody radiation at thermal equilibrium.

It has been proven in [5] that the reduced density matrix of a system interacting with a chaotic bath of bosons, which is well approximated by blackbody radiation, obeys a Lindblad equation (see for example [1–3] and references therein). Here, by using a Lindblad-based approach (LBA) [6,7], we analyze the thermalization process of the LMG model embedded in blackbody radiation. The analysis suggests that complete thermal equilibrium can be reached only at high enough density, while a partial thermalization takes place at low density. In the latter case, along the thermalization process, the total angular momentum remains a conserved quantum number. We then specialize the analysis of the thermalization in this low-density regime, where the total spin is conserved. In the isotropic case, we provide a comprehensive picture of the characteristic thermalization times, as functions of the

Hamiltonian parameters and of the system size N. Quite importantly, we find that these characteristic times diverge with N only at the critical point and in its ferromagnetic phase, linearly at high temperatures, and quadratically at zero temperature. The latter result is to be compared with the time estimated for reaching the ground state of this model by a quantum adiabatic algorithm, which is known to diverge with N^3 [8].

The LMG is a fully connected model of quantum spins which, in the thermodynamic limit, is exactly solvable. It has been the subject of many works, at equilibrium [9,10], along dynamics after a fast quench [11,12], along adiabatic dynamics [13], and in the microcanonical framework [14]. The LMG model has also been used to represent an environment of interacting spins in contact with a system made of a single spin or two spins, by mean-field approximations [15,16], and also by exact numerical analysis of the reduced density matrix [17,18]. The LMG model can find an approximated experimental realization in certain ferroelectrics, ferromagnets [19,20], and magnetic molecules [21]. In more recent years, the model has attracted renewed attention due to the possibility to be simulated by trapped ions [22], as well as by Bose-Einstein condensates of ultracold atoms [23]. Indeed it has been studied experimentally on several platforms: with trapped ions [24,25], with Bose-Einstein condensates via atom-atom elastic collisions [26,27], and via off-resonance atom-light interaction in an optical cavity [28,29]. LMG emerges also as a fully blockaded limit of Rydberg dressed atoms [30] in lattices [31–33], which could have interesting applications to quantum metrology [34–36] as well as to simulation of magnetic Hamiltonians [37,38]. As we discuss more in detail below, LMG can also appear as a coarse-grained model for electric or magnetic quantum dipoles [39].

In the present work, we assume that the components of the LMG system in interaction with a blackbody radiation are actual spins, like in the ferromagnetic compounds, whereas trapped ions and ultracold condensates, even if they behave as

effective spins, can interact with blackbody radiation via other degrees of freedom.

The paper is organized as follows. In Sec. II, we briefly describe our LBA approach to thermalization. The LBA scheme is then specialized in Sec. III, where the environment is chosen to be blackbody radiation. In Sec. IV, we recall the definition of the LMG model. In Sec. V, we investigate under which conditions a description via a LMG model of spins interacting with a blackbody environment is correct, and when the fully coherent limit is valid or not, via tuning of the particle density. In Sec. VI, we derive a simple selection rule that takes place when the fully coherent limit is realized. In Sec. VII, we analyze the isotropic LMG model. Here, we specialize to the fully coherent limit, where the total angular momentum remains conserved, and derive analytically all the elements necessary to evaluate the thermalization times. For the latter, we first provide simple analytical evaluations of both the decoherence and dissipation times, which are then confirmed in Sec. VIII, where we provide a complete numerical analysis, allowing also for a clear picture of the finite-size effects, particularly strong near the critical point. Finally, several crucial conclusions are drawn.

II. THERMALIZATION VIA LINDBLAD EQUATION

Let us consider a system described by a Hamiltonian operator $\boldsymbol{H}$ acting on a Hilbert space $\mathscr{H}$ of dimension M. We assume that the eigenproblem, $\boldsymbol{H}|m\rangle = E_m|m\rangle$, has discrete nondegenerate eigenvalues and that the eigenstates $\{|m\rangle\}$ form an orthonormal system in $\mathscr{H}$. We arrange the eigenvalues in ascending order $E_1 < E_2 < \cdots < E_M$.

In the following we briefly resume our recently proposed LBA to the thermalization of many-body systems with nondegenerate spectra, which allows for an unambiguous definition of the thermalization times, also for compounds of, possibly equal, noninteracting systems [6].

The Lindblad equation (LE) represents the most general class of evolution equations of the reduced density matrix operator $\boldsymbol{\rho}(t)$ of a system interacting with an environment under the assumptions that this evolution is a semigroup and preserves Hermiticity, positivity, and the trace of $\boldsymbol{\rho}(t)$ at all times. The generic LE equation can be written as

$$\frac{d\boldsymbol{\rho}}{dt} = -\frac{i}{\hbar}[\boldsymbol{H}',\boldsymbol{\rho}] + \sum_{\alpha}\left(\boldsymbol{L}_{\alpha}\boldsymbol{\rho}\boldsymbol{L}_{\alpha}^{\dagger} - \frac{1}{2}\{\boldsymbol{L}_{\alpha}^{\dagger}\boldsymbol{L}_{\alpha},\boldsymbol{\rho}\}\right). \quad (1)$$

In this equation, the coherent part of the evolution is represented by the Hermitian operator $\boldsymbol{H}'$ which, in general, differs from the isolated system Hamiltonian $\boldsymbol{H}$. The Lindblad, or quantum jump, operators $\boldsymbol{L}_{\alpha}$ are, for the moment, completely arbitrary operators. Even their number is arbitrary but can always be reduced to $M^2 - 1$. If $\boldsymbol{H}$ has a nondegenerate spectrum, one can represent the most general set of these operators by dyadic products of eigenstates of $\boldsymbol{H}$, namely, $\ell_{m,n}|m\rangle\langle n|$. The meaning of the coefficients $\ell_{m,n}$ is obtained by further developing the theory. When it is imposed that the stationary condition of the system coincides with the Gibbs state, $\boldsymbol{\rho}_G \propto \exp(-\beta\boldsymbol{H})$, for a given inverse temperature β, the Lindblad equation, projected onto the eigenstates of $\boldsymbol{H}$, benefits from a decoupling between the M diagonal terms,

$\rho_{n,n}$, and the $M(M-1)$ off-diagonal terms, $\rho_{m,n}, m \neq n$, and, furthermore, the latter terms are decoupled.

Diagonal terms (Pauli equation). The diagonal terms obey the following master equation:

$$\frac{dp_m(t)}{dt} = \sum_n [p_n(t)W_{n\to m} - p_m(t)W_{m\to n}], \quad (2)$$

where $W_{m\to n} = |\ell_{n,m}|^2$ is the rate probability by which, due to the interaction with the environment, a transition $|m\rangle \to |n\rangle$ occurs. In the weak-coupling limit, these rates can be calculated by using the time-dependent perturbation theory. The above Pauli equation can be written in vectorial form as follows:

$$\frac{d\boldsymbol{p}(t)}{dt} = -\boldsymbol{A}\ \boldsymbol{p}(t), \quad (3)$$

where $p_n = \rho_{n,n}$ and

$$A_{m,n} = \begin{cases} -W_{n\to m}, & m \neq n, \\ \sum_{k\neq m} W_{m\to k}, & m = n. \end{cases} \quad (4)$$

Off-diagonal terms (decoherences). The $M(M-1)$ elements $\rho_{m,n}, m \neq n$, behave as normal modes which relax to zero according to

$$|\rho_{m,n}(t)| = |\rho_{m,n}(0)|e^{-t/\tau_{m,n}}, \quad (5)$$

where

$$\tau_{m,n} = \left[\frac{1}{2}\sum_k (W_{m\to k} + W_{n\to k})\right]^{-1}. \quad (6)$$

The environment is supposed to remain in its own thermal equilibrium at inverse temperature β. Mathematically, this information is encoded in the fact that the matrix $W_{m\to n}$ is similar to a symmetric matrix $C_{m,n}$ having non-negative elements via the square root of the Boltzmann factors $\exp(-\beta E_m)$ and $\exp(-\beta E_n)$, namely,

$$e^{-\frac{\beta}{2}E_m}W_{m\to n}e^{\frac{\beta}{2}E_n} = C_{m,n}. \quad (7)$$

If the transition rates $W_{m\to n}$ satisfy Eq. (7) for some matrix $C_{m,n}$ with $C_{m,n} = C_{n,m} \geqslant 0$, then the stationary state of the LE coincides with the Gibbs state $\boldsymbol{\rho}_G$; i.e., the stationary solution of the Pauli Eq. (2) is $p_m = e^{-\beta E_m}/Z$, where $Z = \sum_k e^{-\beta E_k}$, and $\rho_{m,n} = 0, m \neq n$.

The characteristic time τ by which the system reaches the stationary state is thus due to two different processes:

$$\tau = \max\{\tau^{(P)}, \tau^{(Q)}\}, \quad \text{thermalization time}, \quad (8a)$$

$$\tau^{(P)} = \frac{1}{\mu_2(\boldsymbol{A})}, \quad \text{dissipation time}, \quad (8b)$$

$$\tau^{(Q)} = \max_{m\neq n} \tau_{m,n}, \quad \text{decoherence time}. \quad (8c)$$

The matrix $\boldsymbol{A}$ associated with the Pauli Eq. (2) has a unique zero eigenvalue and $M - 1$ positive eigenvalues [7]. In the above definition of $\tau^{(P)}$, $\mu_2(\boldsymbol{A})$ is the smallest nonzero eigenvalue of $\boldsymbol{A}$. The natural interpretation of $\tau^{(P)}$ is that it represents a characteristic time by which the system loses or gains energy, whereas $\tau^{(Q)}$ represents a characteristic time by which the system loses quantum coherence.

The above LBA satisfies a series of minimal physical requirements, as evident when applied to the case in which the environment is a blackbody radiation, which will be briefly illustrated in the next section. We stress that the remarkable simplicity of our equations is not due to some heuristic approach: they originate uniquely from the Lindblad class when the Gibbs stationary state is imposed. The LBA is equivalent to the popular quantum optical master equation (QOME) [1], only when there is no degeneracy in the energy levels as well as in the energy gaps of $\boldsymbol{H}$ [6]. As we shall show later, when we consider the subspace where the total angular momenta $\boldsymbol{J}^2$ is fixed, in the LMG model the energy levels as well as the energy gaps are nondegenerate [see Eq. (37)]. Therefore, in the subspace where $\boldsymbol{J}^2$ is fixed, all the results that we obtain could be equally derived from the QOME.

III. BLACKBODY RADIATION

In the case in which the environment is blackbody radiation at inverse temperature β, the time-dependent perturbation theory combined with the Planck law yields (this result can be reached by treating the electromagnetic field classically, provided at the end the contribution due to the spontaneous emission is added)

$$A_{m,m} = \sum_{k:\, E_k < E_m} D_{k,m} \frac{(E_m - E_k)^3}{1 - e^{-\beta(E_m - E_k)}}$$
$$+ \sum_{k:\, E_k > E_m} D_{k,m} \frac{(E_k - E_m)^3}{e^{\beta(E_k - E_m)} - 1}, \qquad (9)$$

whereas the off-diagonal terms $m \neq n$ of $\boldsymbol{A}$ are

$$A_{m,n} = \begin{cases} -D_{m,n} \frac{(E_m - E_n)^3}{e^{\beta(E_m - E_n)} - 1}, & E_m > E_n, \\ 0, & E_m = E_n, \\ -D_{m,n} \frac{(E_n - E_m)^3}{1 - e^{-\beta(E_n - E_m)}}, & E_m < E_n. \end{cases} \qquad (10)$$

The coefficients $D_{m,n}$ are magnetic or electric dipole matrix elements, whose value depends on the properties of the system embedded in the blackbody radiation as follows. In the following, we focus on the case in which the system interacts with the electromagnetic (EM) field through magnetic dipole operators $\mu\boldsymbol{\sigma}_i = (\mu\sigma_i^x, \mu\sigma_i^y, \mu\sigma_i^z)$, where the index i labels the individual elements of the system located at position $\boldsymbol{r}_i$. All the dynamics is encoded in the internal degrees of freedom; therefore all the particles are considered fixed in space. Based on the analysis of [40] the thermalization dynamics is characterized by three regimes:

Fully coherent regime. If the following condition holds,

$$|E_n - E_m| \ll hc/\ell, \quad \ell = \max_{i \neq j} |\boldsymbol{r}_i - \boldsymbol{r}_j|, \qquad (11)$$

then the following formula applies,

$$D_{n,m} = \gamma \sum_{h=x,y,z} \left| \langle n| \sum_{i=1}^N \sigma_i^h |m\rangle \right|^2, \qquad (12)$$

where the coupling constant γ, in Gaussian units, can be expressed in terms of the magnetic dipole operator and

fundamental constants as

$$\gamma = \frac{4\mu^2}{3\hbar^4 c^3}. \qquad (13)$$

For $N = 1$, Eq. (12) equals the standard textbook formula based on the long-wavelength approximation [41].

Fully incoherent regime. If the following condition holds,

$$|E_n - E_m| \gg hc/a, \quad a = \min_{i \neq j} |\boldsymbol{r}_i - \boldsymbol{r}_j|, \qquad (14)$$

then the following formula applies,

$$D_{n,m} = \gamma \sum_{i=1}^N \sum_{h=x,y,z} \left| \langle n|\sigma_i^h|m\rangle \right|^2. \qquad (15)$$

Since $hc = 1.23$ eVμm, we have that for atomic or molecular systems in which $|E_n - E_m|$ is typically of a few eV and ℓ is not larger than a few tens of Å, condition (11) is well satisfied. Instead, for microscopic systems in which a is 1 μm and the energy-level separations $|E_n - E_m|$ are much larger than the atomic eV scale, condition (14) applies.

Concerning the incoherent limit, from Eqs. (9) and (10) we see that, even if for some pairs of states $|m\rangle, |n\rangle$ the condition (14) is not satisfied, the contribution corresponding to such pairs can be neglected if $\beta \Delta E \ll 1$, where ΔE is the largest of the values $|E_n - E_m|$ for which the condition (14) does not hold. From Eq. (14) we see that a sufficient condition for this to occur is

$$\beta hc/a \ll 1. \qquad (16)$$

Intermediate regime. When none of the above inequalities (11), (14), and (16) hold, there is no simple formula to be applied, and one should include contributions with mixed dipole matrix elements. These contributions originate from the general formula for the transition probabilities of a many-body system perturbed by the presence of the blackbody radiation [40]:

$$P_{n,m}^{\pm} = \frac{\mu^2}{2\pi\hbar c^3} \frac{\omega_{n,m}^3}{e^{\hbar\omega_{n,m}/k_B T} - 1} \sum_{i=1}^N \sum_{j=1}^N \sum_{h=1}^3 \sum_{l=1}^3 Q_{n,m}^{i,j;h,l}$$
$$\times \langle E_n|\sigma_i^h|E_m\rangle \overline{\langle E_n|\sigma_j^l|E_m\rangle}, \qquad (17)$$

where

$$\omega_{n,m} = |E_n - E_m|/\hbar \qquad (18)$$

and

$$Q_{n,m}^{i,j;h,l} = \int_0^\pi \sin\theta d\theta \int_0^{2\pi} d\phi \, e^{i\boldsymbol{u}\cdot(\boldsymbol{r}_i - \boldsymbol{r}_j)\omega_{n,m}/c}(\delta_{h,l} - u_h u_l), \qquad (19)$$

with $\boldsymbol{u} = (\sin\theta\cos\phi, \sin\theta\sin\phi, \cos\theta)$. Equation (17) interpolates between the fully coherent and fully incoherent limits. Later on, we shall make use of Eq. (17) to show that, in the LMG model, as soon as condition (11) is not satisfied, $\boldsymbol{J}^2$ is not conserved.

IV. THE LIPKIN-MESHKOV-GLICK MODEL

Let us consider the Hilbert space $\mathcal{H}$ of N spins $S = \sigma\hbar/2$, where $\boldsymbol{\sigma} = (\sigma^x, \sigma^y, \sigma^z)$ are the standard Pauli matrices. The

dimension of $\mathcal{H}$ is $M = 2^N$. The LMG model is defined in $\mathcal{H}$ through the Hamiltonian

$$H = -\frac{\mathcal{J}\hbar^2}{4N} \sum_{i \neq j}^{N} \left(\sigma_i^x \sigma_j^x + \gamma_y \sigma_i^y \sigma_j^y\right) - \frac{\Gamma\hbar}{2} \sum_{i=1}^{N} \sigma_i^z, \quad (20)$$

where $\mathcal{J}$ is the spin-spin coupling, Γ the strength of a transverse field, and γ_y the so-called anisotropy parameter. The model is known to provide an exactly solvable mean-field-like behavior in the limit $N \to \infty$ [4]. Let us introduce the components $h = x, y, z$ of the total spin operator $\boldsymbol{J}$:

$$J_h = \frac{\hbar}{2} \sum_{i=1}^{N} \sigma_i^h. \quad (21)$$

Up to the additive constant $\mathcal{J}\hbar^2(1 + \gamma_y)/4$, we can rewrite the Hamiltonian as

$$H = -\frac{\mathcal{J}}{N}\left(J_x^2 + \gamma_y J_y^2\right) - \Gamma J_z. \quad (22)$$

It follows that $[\boldsymbol{H}, \boldsymbol{J}^2] = 0$ and $[\boldsymbol{H}, \prod_i \sigma_i^z] = 0$. These two relations imply, whenever the system of N spins is isolated, the conservation of the total spin $\boldsymbol{J}^2$, and the conservation of the parity along the z direction. As a consequence, the eigenstates $|m\rangle$ of $\boldsymbol{H}$ can be chosen as (the label m here should not be confused with the eigenvalues of J_z, for which we shall use the symbol m_z)

$$|m\rangle = |j, p, \alpha\rangle \in \mathcal{H}_j \cap \mathcal{H}^{(p)}, \quad (23)$$

where j is the quantum number associated with $\boldsymbol{J}^2$, i.e., $\boldsymbol{J}^2|j, p, \alpha\rangle = \hbar^2 j(j+1)|j, p, \alpha\rangle$, and $p = \pm 1$ is the parity, i.e., $\prod_i \sigma_i^z |j, p, \alpha\rangle = p|j, p, \alpha\rangle$. The Greek symbol α stands for a suitable set of quantum numbers that allow the state $|j, p, \alpha\rangle$ to span the intersection between the $2j + 1$ dimensional Hilbert space $\mathcal{H}_j$, where j is fixed, and the $2^N/2$ dimensional Hilbert space $\mathcal{H}^{(p)}$, known as the "half space" of $\mathcal{H}$ in which p is fixed. According to the rules for the addition of angular momenta, for N spins 1/2 we have

$$N \text{ odd} \Rightarrow j \in \{1/2, 3/2, \ldots, N/2\}, \quad (24a)$$

$$N \text{ even} \Rightarrow j \in \{0, 1, \ldots, N/2\}. \quad (24b)$$

In the symmetric case, $\gamma_y = 1$, we also have $[\boldsymbol{H}, J_z] = 0$, and the index pair (p, α) coincides with (p, m_z), where m_z is the eigenvalue of $J_z/\hbar$, taking the values $-j, -j+1, \ldots, j$ restricted to either $p = 1$ or $p = -1$ (if two values m_z and m_z' have the same parity, then $|m_z' - m_z|$ can be either 0 or 2).

V. IMPLEMENTATIONS OF LMG WITH MAGNETIC SYSTEMS IN A BLACKBODY ENVIRONMENT

In this section, we want to analyze which regime, fully coherent, fully incoherent, or intermediate, takes place in realistic models characterized by an effective LMG description. We restrict ourselves to two magnetic systems with permanent magnetic moment. A more general analysis devoted to the study of atomic and molecular systems with electric dipole moments will be done somewhere else.

In general, the conditions (11) or (14) must be checked for all those pairs (m, n) of eigenstates contributing with nonzero

dipole elements (12) and (15). However, in the LMG model, as well as in models characterized by a smooth energy landscape, near states correspond to near energies and, moreover, since the operators associated with the dipole matrix elements are sums of Pauli matrices, the dipole matrix elements can connect only states that differ by single spin flips. Therefore, the pairs (m, n) for which we have to control the conditions (11) or (14), with respect to possible dependencies on N, always have $|E_n - E_m| \sim \mathcal{J}\hbar^2$.

The first realistic model of interest is provided by the so-called high-spin molecules. These are large molecules having a large total spin j (which defines the eigenvalues of $\boldsymbol{J}^2$), well described by the LMG Hamiltonian (22). According to Ref. [21], in the high-spin molecule Mn_{12}, we have $j = 10$ and $hc/(\mathcal{J}\hbar^2) \simeq 2$ cm. Substituting the latter value in Eq. (11), we see that the fully coherent condition becomes $\ell \ll 2$ cm, which is certainly satisfied (the diameter of the molecule cannot overcome a few tens of angstroms).

The other class of realistic models concerns magnetic ions in a crystalline environment, such as $Dy(C_2H_5SO_4)_3 9H_2O$ and $DyPO_4$, among others [19,20], and ultracold atoms with a permanent dipole moment [39]. Here, the dipole-dipole interaction decays with the cube of the distance between two neighboring ions and is anisotropic. As a consequence, unless the temperature is sufficiently high, as prescribed by Eq. (16), there is no way to stay in the fully incoherent regime. This becomes clear by the following argument. Two neighboring spins S_i and S_j interact via the dipole-dipole Hamiltonian:

$$H_{i,j} = -\frac{\mu_0}{4\pi |\mathbf{r}|^3} \left[3(\mathbf{m}_1 \cdot \mathbf{r})(\mathbf{m}_2 \cdot \mathbf{r})\frac{1}{|\mathbf{r}|^2} - \mathbf{m}_1 \cdot \mathbf{m}_2\right], \quad (25)$$

where μ_0 is the vacuum permeability, $\mathbf{m}_1$ and $\mathbf{m}_2$ the magnetic moments of the two spins, and $|\mathbf{r}| = a$ their distance. Equation (25) allows us to estimate the coupling constant $\mathcal{J}$ in a coarse-grained Ising-like Hamiltonian for spin-1/2 particles $H = -\sum_{(i,j)} \mathcal{J} S_i S_j$. In fact, if each magnetic moment has an electronic origin, we have $|\mathbf{m}_i| \sim \mu_B$, where μ_B is the Bohr magneton. By comparison between $\mathcal{J} S_i S_j$ and $H_{i,j}$, we can rewrite the Ising coupling in terms of fundamental constants as

$$\mathcal{J}\hbar^2 \sim \alpha^3 a_0^2 \frac{\pi \hbar c}{a^3}, \quad (26)$$

where α_0 is the fine-structure constant, and a_0 is the Bohr radius. We can now apply Eq. (26) to condition (11) and find that the fully coherent condition amounts to

$$\alpha^3 a_0^2 \ll \frac{a^3}{\ell}, \quad (27)$$

while applying Eq. (26) to condition (14) we see that the fully incoherent condition amounts to

$$\alpha^3 a_0^2 \gg a^2. \quad (28)$$

Since $a \geqslant a_0$ and $\alpha \simeq 1/137$, we see that Eq. (28) is never satisfied. Equation (27) can be instead satisfied at sufficiently low densities. In fact, since $\ell \sim aN^{1/d}$, where d is the dimension (real or effective) of the system, we see that Eq. (27) is satisfied if a grows with N at least as $a \sim a_0 N^{1/(2d)}$. Whereas for finite d such a condition amounts, in the thermodynamic limit, to infinitely small densities, for $d = \infty$, such as occurs in a fully connected model, Eq. (27) is certainly satisfied for

any finite density. However, the fully connected interaction is a theoretical extrapolation, as the actual d will remain finite. In this sense, we can consider the LMG model as a mean-field approximation of the finite-dimensional case. As a consequence, we expect that some trade-off will take place, with the fully coherent limit being satisfied only for densities lower than some threshold. The numerical value of this threshold could be calculated on the basis of the specific limiting procedure $d \to \infty$ chosen for defining the LMG model, which is beyond the aim of the present work. In any case, a threshold exists, and for densities higher than the threshold, neither Eq. (27) and nor Eq. (28) are satisfied, and the general formula (17) should be applied instead. In the next section, we will make use of the general formula (17) to show that, along the thermalization, whenever the fully coherent regime is not satisfied, as occurs at high densities, the total angular momentum is not conserved, while, for the rest of the paper, we will perform a comprehensive analysis of the thermalization by assuming the fully coherent regime, as is expected to take place at low densities.

VI. SELECTION RULES FOR THE THERMALIZATION OF THE LMG MODEL

To determine the matrix elements of $\boldsymbol{A}$ from Eqs. (9) and (10), one must evaluate the dipole matrix elements $D_{m,n}$. Let us indicate by $|m\rangle = |j,p,\alpha\rangle$ and $|n\rangle = |j',p'\alpha'\rangle$ two generic eigenstates of $\boldsymbol{H}$. Since $[\boldsymbol{J}^2, J_h] = 0$, for any $h = x,y,z$, we clearly have

$$J_h|m\rangle = J_h|j,p,\alpha\rangle \in \mathcal{H}_j, \tag{29}$$

so that, if we assume the fully coherent regime, from Eq. (12), for dipole matrix element we have

$$D_{m;n} = D_{j,p,\alpha;j',p',\alpha'} = 0 \quad \text{if } j \neq j'. \tag{30}$$

Furthermore, whereas J_z conserves the parity, this is not true for J_x and J_y, so that, in general, we also have

$$D_{m;n} = D_{j,p,\alpha;j,p',\alpha'} \neq 0. \tag{31}$$

Let us consider now the fully incoherent regime. Consider, for example, the symmetric case $\gamma_y = 1$, where $|j,p,\alpha\rangle = |j,p,m_z\rangle$ and choose $N = 2$. The basis is spanned by the singlet state $j = 0$, $m_z = 0$ and the triplet states $j = 1$, $m_z = -1,0,+1$. From Eq. (15), we see that the dipole matrix elements contain, for example, contributions proportional to

$$\left|\langle j=1,p,m_z=1|\sigma_1^z|j=0,p',m_z=0\rangle\right| = 0, \tag{32}$$

$$\left|\langle j=1,p,m_z=1|\sigma_1^x|j=0,p',m_z=0\rangle\right|$$
$$= \left|\langle j=1,p,m_z=1|\sigma_1^y|j=0,p',m_z=0\rangle\right| \neq 0, \tag{33}$$

(and similarly for σ_2^h, $h = x,y,z$), which give

$$D_{m;n} = D_{j,p,\alpha;j',p',\alpha'} \neq 0, \quad \text{even if } j \neq j'. \tag{34}$$

Finally, let us consider the intermediate regime, and for simplicity let us again consider a system with $N = 2$. From the right-hand side of the general formula (17), we see that, in particular, the contributions corresponding to the case $i = j$ and $h = l$ are proportional to the terms (32) and (33) and alike.

Equations (30), (31), and (34) show that whereas the thermalization process is always able to connect states with different parity, in the fully coherent regime the thermalization process does not connect states with different total spin, whereas it is able to do so outside of this regime.

In the following, we will disregard the description of the states in terms of p and we shall use the notation $|j,\alpha\rangle$ since, regardless of the regime, the parity of the state does not provide any useful selection rule.

VII. THERMALIZATION IN THE FULLY COHERENT REGIME FOR ISOTROPIC LMG MODELS

In the fully coherent limit, if the system is initially prepared in a mixture, $\boldsymbol{\rho}_j(t = 0)$, of eigenstates of $\boldsymbol{J}^2$, all with eigenvalues j, it will remain in the subspace $\mathcal{H}_j$ for all times. In other words, the system will undergo a partial thermalization, reaching asymptotically the following thermal state:

$$\lim_{t\to\infty} \boldsymbol{\rho}_j(t) = \frac{\exp(-\beta\boldsymbol{H})\boldsymbol{P}_j}{Z_j}, \tag{35}$$

where $\boldsymbol{P}_j$ is the projector onto $\mathcal{H}_j$, and $Z_j = \text{tr}[\exp(-\beta\boldsymbol{H})\boldsymbol{P}_j]$.

We now briefly review the properties of the isotropic LMG model and discuss in detail its thermalization properties. If $\gamma_y = 1$, the Hamiltonian (22) simplifies as

$$\boldsymbol{H} = -\frac{\mathcal{J}}{N}J^2 + \frac{\mathcal{J}}{N}J_z^2 - \Gamma J_z, \tag{36}$$

where, as long as we are confined in the subspace $\mathcal{H}_j$, the first term is a constant. Note that whereas in the full Hilbert space $\mathcal{H}$ the Hamiltonian Eq. (36) leads to a ferromagnetic phase, in $\mathcal{H}_j$, if $\mathcal{J} > 0$, as usually assumed in the LMG models, Eq. (36) represents the classical Hamiltonian of a fully connected Ising model with an antiferromagnetic coupling, a highly frustrated system with no ordinary finite-temperature phase transition. Therefore, a phase transition can occur in the LMG model only at zero temperature, and the order parameter must be properly defined [9]. In order to have some magnetization in $\mathcal{H}_j$ with a finite-temperature phase transition, one must allow γ_y to be different from 1. An explicit classical analysis of the finite-temperature phase transition can be found in [11]. We stress that, even if, for $\gamma_y = 1$, the Hamiltonian (22) is somehow classical, its thermalization is governed by genuine quantum processes. More precisely, the interaction with the surrounding EM field is not trivial since all three components of the total spin participate.

Below we provide an exact analysis of the thermalization of the LMG model for $\gamma_y = 1$. We first analyze the static and equilibrium properties, and then calculate the dipole matrix elements which, in turn, allow us to evaluate the thermalization times by using the equations discussed in Secs. II and III.

A. Energy levels, gap, and critical point

In the following we will work in units where $\hbar = 1$. If $\gamma_y = 1$, the eigenstates of the Hamiltonian $\boldsymbol{H}$ are simply given by $|m\rangle = |j,m_z\rangle$, with eigenvalues

$$E(j,m_z) = -\frac{\mathcal{J}j(j+1)}{N} + m_z\left(\frac{\mathcal{J}m_z}{N} - \Gamma\right), \tag{37}$$

with $m_z \in \{-j, -j+1, \ldots, j\}$. We assume $N \geqslant 2$. Furthermore, we consider $j > 0$; otherwise there exists only one state $|j = 0, m_z = 0\rangle$. As a consequence, we have $j \geqslant 1$ integer if N is even or semi-integer if N is odd.

From Eq. (37) we have [hereafter, since j is fixed, we use the shorter notation $E_{m_z} = E(j, m_z)$]

$$E_{m_z} - E_{m_z-1} = \frac{(2m_z - 1)\mathcal{J} - \Gamma N}{N}, \quad m_z \geqslant -j+1, \quad (38a)$$

$$E_{m_z} - E_{m_z+1} = \frac{\Gamma N - (2m_z + 1)\mathcal{J}}{N}, \quad m_z \leqslant j-1. \quad (38b)$$

In the following, we indicate by $m_z^{(1)}$ the ground state (GS), and by $m_z^{(2)}$ the first excited state (FES). Let us suppose for the moment that $\Gamma N/(2\mathcal{J})$ is not a half integer for j even (is not an integer for j odd) so that, even for N finite, the gaps do not close. For the GS, we have

$$E_{m_z^{(1)}} = \min_{m_z} E_{m_z}, \quad m_z^{(1)} = \mathrm{sgn}(\Gamma) \min \left\{ \left[\frac{|\Gamma| N}{2\mathcal{J}} \right]_j, j \right\}, \quad (39)$$

where we have defined

$$[x]_j = \begin{cases} \text{integer closest to } x, & j \text{ even,} \\ \text{semi-integer closest to } x, & j \text{ odd.} \end{cases} \quad (40)$$

It is convenient to introduce

$$\delta = \left[\frac{\Gamma N}{2\mathcal{J}} \right]_j - \frac{\Gamma N}{2\mathcal{J}}. \quad (41)$$

By using Eqs. (37) and (39), and the definition of δ, for the GS and FES levels we obtain

$$E_{m_z^{(1)}} = \begin{cases} -\frac{\mathcal{J}j(j+1)}{N} - \frac{\Gamma^2 N}{4\mathcal{J}} + \frac{\mathcal{J}\delta^2}{N}, & \Gamma/\mathcal{J} \in \left[-\frac{2(j-\delta)}{N}, \frac{2(j-\delta)}{N} \right], \\ -\frac{\mathcal{J}j(j+1)}{N} + \frac{\mathcal{J}j^2}{N} - j|\Gamma|, & \Gamma/\mathcal{J} \notin \left[-\frac{2(j-\delta)}{N}, \frac{2(j-\delta)}{N} \right], \end{cases} \quad (42)$$

$$E_{m_z^{(2)}} = \min_{m_z \neq m_z^{(1)}} E_{m_z} = \begin{cases} E_{m_z^{(1)}-\mathrm{sgn}(\delta)}, & |m_z^{(1)} - \mathrm{sgn}(\delta)| \leqslant j, \\ E_{m_z^{(1)}+\mathrm{sgn}(\delta)}, & |m_z^{(1)} - \mathrm{sgn}(\delta)| > j \text{ and } |m_z^{(1)} + \mathrm{sgn}(\delta)| \leqslant j, \\ E_{\mathrm{sgn}(\Gamma)(j-1)}, & m_z^{(1)} = \mathrm{sgn}(\Gamma)j. \end{cases} \quad (43)$$

From Eqs. (38)–(43) we evaluate the first gap Δ:

$$\Delta = E_{m_z^{(2)}} - E_{m_z^{(1)}} = \begin{cases} |\Gamma| - \mathcal{J}\frac{2j-1}{N}, & \frac{\Gamma}{\mathcal{J}} \notin \left[-\frac{2(j-\delta)}{N}, \frac{2(j-\delta)}{N} \right], \\ \mathcal{J}\frac{1+2|\delta|}{N}, & \frac{\Gamma}{\mathcal{J}} \in \left[-\frac{2(j-\delta)}{N}, -\frac{2[j-r(\delta)-\delta]}{N} \right] \cup \left[\frac{2[j-r(\delta)-\delta]}{N}, \frac{2(j-\delta)}{N} \right], \\ \mathcal{J}\frac{1-2|\delta|}{N}, & \frac{\Gamma}{\mathcal{J}} \in \left[-\frac{2[j-r(\delta)-\delta]}{N}, \frac{2[j-r(\delta)-\delta]}{N} \right], \end{cases} \quad (44)$$

where $r(\delta) = 1$ if $\delta\Gamma < 0$ and $r(\delta) = 0$ otherwise. If $r(\delta) = 0$, the intermediate intervals in the second line of Eq. (44) are empty sets. Equation (44) shows that, for N finite, we can define two "exact critical points", Γ_c^+ and Γ_c^-, as solutions, respectively, of the equations

$$\frac{\Gamma_c^\pm}{\mathcal{J}} = \pm 2 \frac{(j-\delta)}{N}. \quad (45)$$

By using the definition of δ, it is easy to check that, for any N, Eqs. (45) are solved for Γ such that $\delta = 0$, i.e.,

$$\frac{\Gamma_c^\pm}{\mathcal{J}} = \pm \frac{\Gamma_c}{\mathcal{J}} = \pm \frac{2j}{N}. \quad (46)$$

Notice that, for j even (odd), the function $[x]_j$ has two values for x semi-integer (integer). For j even this reflects the fact that, whenever $\Gamma N/(2\mathcal{J}) = k/2$, for some odd (even, if j is odd) integer k such that $|k/2 \pm 1/2| < j$, the GS level can be twofold degenerate, with the states $m_z^{(1a)} = k/2 - 1/2$ and $m_z^{(1b)} = k/2 + 1/2$. The general expression of the GS, as well as of the FES, for the case in which $\Gamma N/(2\mathcal{J})$ is semi-integer for j even (or integer for j odd) is cumbersome. It is however clear that such a condition on the external field Γ is of no physical interest, since one can approach an integer or a semi-integer by an infinite sequence of real numbers that are neither integer nor half integer.

Equation (44) shows that there is an inner region in Γ where the gap closes to zero as $\Delta = (1 - 2|\delta|)\mathcal{J}/N$, a paramagnetic external region where Δ remains finite, and a transient region, whose size tends to zero as $1/N$ and $\Delta = (1 + 2|\delta|)\mathcal{J}/N$.

Finally, we point out that analogous formulas hold for the successive gaps. For example, for the difference between the third and the second energy level, Δ', there is an interval in Γ where Δ' goes to zero as $1/N$, and, for N large, such interval and gap differ for negligible terms from, respectively, the interval and gap between GS and FES.

B. Partition function

For later use, we also calculate the partition function Z_j for j large of the type $j = \alpha N$, with α constant. From Eq. (37) we have

$$Z_j = e^{\frac{\beta \mathcal{J} j(j+1)}{N}} \sum_{m_z \in [-j, -(j-1), \ldots, j]} e^{\beta N m_z \left(\frac{\mathcal{J} m_z}{N} - \Gamma \right)}$$

$$= e^{\frac{\beta \mathcal{J} j(j+1)}{N}} \sum_{x \in [-1, -(j-1)/j, \ldots, 1]} e^{\beta \alpha x N(\mathcal{J} \alpha x - \Gamma)}. \quad (47)$$

For large N, the above sum can be approximated by an integral over the range $(-1, 1)$, and we get

$$Z_j = \sqrt{\frac{2\pi N}{\beta J \alpha^2}} e^{\frac{\beta \mathcal{J} j(j+1)}{N}} e^{\beta \Gamma \frac{\Gamma N}{2\mathcal{J}}} \left[1 + O\left(\frac{1}{N} \right) \right]. \quad (48)$$

Notice the absence of the constant α in the second exponential.

C. Dipole matrix elements

In order to evaluate the dipole matrix elements, we shall make use of the ladder operators $J_{\pm} = J_x \pm i J_y$. Let us consider two generic eigenstates $|m\rangle = |j, m_z\rangle$ and $|n\rangle = |j, n_z\rangle$, with $m_z, n_z \in \{-j, -j+1, \ldots, j\}$. From Eq. (12), by using $D_{m,n} = \gamma \sum_h |\langle j, m_z | 2 J^h | j, n_z \rangle|^2$, we have

$$D_{m_z, n_z} = 2\gamma \left[(j - n_z)(j + n_z + 1)\delta_{m_z, n_z+1} + (j + n_z)(j - n_z + 1)\delta_{m_z, n_z-1} \right]. \tag{49}$$

By plugging Eq. (49) into Eqs. (9) and (10), with $A_{m,n} = A_{m_z, n_z}$, we get

$$A_{m_z, m_z} = 2\gamma (j - m_z + 1)(j + m_z) f\left(E_{m_z-1} - E_{m_z}\right) + 2\gamma (j + m_z + 1)(j - m_z) f\left(E_{m_z+1} - E_{m_z}\right) \tag{50}$$

and

$$A_{m_z, m_z-1} = -2\gamma (j - m_z + 1)(j + m_z) f\left(E_{m_z} - E_{m_z-1}\right), \tag{51a}$$

$$A_{m_z, m_z+1} = -2\gamma (j + m_z + 1)(j - m_z) f\left(E_{m_z} - E_{m_z+1}\right), \tag{51b}$$

$$A_{m_z, n_z} = 0, \quad n_z \neq m_z, m_z - 1, m_z + 1, \tag{51c}$$

where we have introduced the function $f(E_m)$:

$$f\left(E_{m_z} - E_{n_z}\right) = \frac{\left(E_{m_z} - E_{n_z}\right)^3}{e^{\beta(E_{m_z} - E_{n_z})} - 1} \theta\left(E_{m_z} - E_{n_z}\right) + \frac{\left(E_{n_z} - E_{m_z}\right)^3}{1 - e^{-\beta(E_{n_z} - E_{m_z})}} \theta\left(E_{n_z} - E_{m_z}\right), \tag{52}$$

$\theta(x)$ being the Heaviside step function. Plugging Eqs. (50) into Eqs. (4) and (6), we calculate the decoherence times as

$$\tau_{m_z, n_z} = \left[2\gamma (j - m_z + 1)(j + m_z) f\left(E_{m_z-1} - E_{m_z}\right) + 2\gamma (j + m_z + 1)(j - m_z) f\left(E_{m_z+1} - E_{m_z}\right) \right.$$

$$\left. + 2\gamma (j - n_z + 1)(j + n_z) f\left(E_{n_z-1} - E_{n_z}\right) + 2\gamma (j + n_z + 1)(j - n_z) f\left(E_{n_z+1} - E_{n_z}\right) \right]^{-1}, \quad m_z \neq n_z. \tag{53}$$

In this framework, j is fixed, but it can be chosen to be any value in agreement with Eqs. (24). Notice that, since in Eq. (53) $m_z \neq n_z$, the values $j = 0$ (for N even) and $j = 1/2$ (for N odd) are not allowed (obviously, for such fixed values of j we have no dynamics at all). The decoherence times (53) can be easily evaluated numerically for any choice of the allowed j, m_z, and n_z. Depending on the particular value of Γ, which determines the energy gap Δ via Eq. (44), we can have different thermalization regimes. Below we provide analytical evaluations corroborated by exact numerical results.

D. Decoherence for $\Gamma/\mathcal{J} \notin [-\frac{2(j-\delta)}{N}, \frac{2(j-\delta)}{N}]$

In this case, Δ is finite and, if $\beta\Gamma = O(1)$, from Eqs. (38) we have

$$f\left(E_{m_z \pm 1} - E_{m_z}\right) \sim O\left(\left| \Gamma - \mathcal{J}\frac{2m_z \pm 1}{N} \right|^3\right). \tag{54}$$

By using Eqs. (54) in Eqs. (53), we get the two following possible scaling laws with respect to j:

$$\tau_{m_z, n_z} = O\left(\frac{1}{\gamma |\Gamma|^3 j^2}\right), \quad |m_z|, \text{ or } |n_z| \ll j, \tag{55a}$$

$$\tau_{m_z, n_z} = O\left(\frac{1}{\gamma \left| \Gamma - \mathcal{J}\frac{2j}{N} \right|^3 j}\right), \quad m_z \sim n_z \sim j, \tag{55b}$$

$$\tau_{m_z, n_z} = O\left(\frac{1}{\gamma \left| |\Gamma| + \mathcal{J}\frac{2j}{N} \right|^3 j}\right), \quad m_z \sim j, n_z \sim -j,$$

$$m_z \sim -j, n_z \sim j, \tag{55c}$$

$$\tau_{m_z, n_z} = O\left(\frac{1}{\gamma \left| \Gamma + \mathcal{J}\frac{2j}{N} \right|^3 j}\right), \quad m_z \sim n_z \sim -j. \tag{55d}$$

Equations (55) show that, for a given j, the states which remain coherent for a longer time are those with $m_z \sim n_z \sim \text{sgn}(\Gamma) j$. Quite importantly, Eqs. (55) imply that, if j is fixed and independent of N, the decoherence times do not scale with N at all. Consider in particular the states with $j = 0$. For N even, these states are the sum of all the $N!$ permutations of spin flips with alternate signs, i.e., the N-particle analog of the singlet 2-particle state, an intrinsically entangled state. Equations (55) tell us, if one is able to initially prepare the system with a small value of j, N-entangled states will show a strong resilience to decoherence. From the point of view of thermalization, this reflects on the overall thermalization time $\tau^{(Q)}$, which, from Eqs. (55), becomes

$$\tau^{(Q)} = \max_{m_z \neq n_z} \tau_{m_z, n_z} = O\left(\frac{1}{\gamma \left| |\Gamma| - \mathcal{J}\frac{2j}{N} \right|^3 j}\right). \tag{56}$$

In the limit of zero temperature $\beta \to \infty$, we can exploit

$$\lim_{\beta \to \infty} f\left(E_{m_z} - E_{n_z}\right) = \begin{cases} 0, & E_{m_z} > E_{n_z}, \\ \left(E_{n_z} - E_{m_z}\right)^3, & E_{m_z} < E_{n_z}. \end{cases} \tag{57}$$

By applying Eqs. (57) and (53), we achieve, roughly, the same overall behavior as Eq. (56).

E. Decoherence for $\Gamma/\mathcal{J} \in [-\frac{2(j-\delta)}{N}, \frac{2(j-\delta)}{N}]$

In this case, $\Delta \sim \Delta' \sim \Delta'' \ldots \sim 1/N$. If $\beta\mathcal{J} = O(1)$ and $\beta|\Gamma| = O(1)$, Eqs. (43) and (44) and their generalization for the successive gaps (whose details are not important here) show that

$$f\left(E_{m_z \pm 1} - E_{m_z}\right) \sim O\left(\frac{|\Gamma| \mathcal{J}^2}{N^2}\right). \tag{58}$$

The interval in Γ where Eq. (58) can be applied to the arbitrary state m_z is not trivial. However, observing that Eq. (58) can be applied to the GS and to the FES is enough to claim that, for $\Gamma/\mathcal{J} \in [-\frac{2(j-\delta)}{N}, \frac{2(j-\delta)}{N}]$,

$$\tau^{(Q)} = O\left(\frac{N^2}{\gamma|\Gamma|\mathcal{J}^2[j^2 + j - (\frac{\Gamma N}{2\mathcal{J}})^2 + \frac{|\Gamma|N}{2\mathcal{J}}]}\right), \quad (59)$$

where we have used Eq. (39) for the explicit form of the GS. From Eq. (59) it follows that, if $j = O(N)$, then

$$\tau^{(Q)}|_{\frac{|\Gamma|}{\mathcal{J}} = \frac{2j}{N}} = O\left(\frac{N}{\gamma|\Gamma|^2\mathcal{J}}\right), \quad (60)$$

whereas

$$\tau^{(Q)}|_{\frac{|\Gamma|}{\mathcal{J}} \ll \frac{2j}{N}} = O\left(\frac{1}{\gamma|\Gamma|\mathcal{J}^2}\right). \quad (61)$$

Equations (60) and (61) show that, despite that the gap closes to zero in all the interval $[-\frac{2j}{N}, \frac{2j}{N}]$, the slowdown dynamics takes place only in correspondence with the critical points $\Gamma_c^{\pm}/\mathcal{J} = \pm 2j/N$, and the decoherence time scales only linearly in N. On the other hand, we find it remarkable to notice that, at the critical point, the decoherence time turns out to be a growing function of N. This observation confirms and strengthen the general idea that phase transitions could be exploited to generate resilience to decoherence and large entangled states [15,16].

Notice that Eq. (58) is valid also for β large, provided N is sufficiently large too. However, in general, the limits $\beta \to \infty$ and $N \to \infty$ cannot be switched. If we are interested in $\lim_{N\to\infty} \lim_{\beta\to\infty} \tau_{m_z,n_z}$ we can simply use Eq. (57) applied to Eq. (53). The special case at $\Gamma = \Gamma_c$ will be analyzed later. If instead we are interested in $\lim_{\beta\to\infty} \lim_{N\to\infty} \tau_{m_z,n_z}$ we can use Eqs. (58)–(61) by substituting everywhere one factor $|\Gamma|$ with $1/\beta$. This shows that, in the thermodynamic limit, the thermalization time diverges at least linearly in β.

F. Dissipation

In order to evaluate the dissipation time $\tau^{(P)}$, we must find the eigenvalue $\mu_2(A)$ of the $2j \times 2j$ matrix A given in Eqs. (50) and (51). In general, this can be done only numerically. In the present case, this task is largely simplified because A is a tridiagonal matrix.

From an analytical point of view, we can apply the general rule that, for β finite, $\lim_{N\to\infty} \tau^{(P)} \geqslant \lim_{N\to\infty} \tau^{(Q)}$, with $\tau^{(Q)}$ given by Eqs. (56), (60), and (61). Equation (60), in particular, implies that the thermalization time $\tau = \max\{\tau^{(P)}, \tau^{(Q)}\}$, at the critical point, and β fixed diverges linearly in N. Actually, the rule $\lim_{N\to\infty} \tau^{(P)} \geqslant \lim_{N\to\infty} \tau^{(Q)}$ applies, if [7]

$$\lim_{N\to\infty} \frac{e^{-\beta E(j,m_z^{(1)})}}{Z_j} = 0. \quad (62)$$

Comparing Eq. (42) with Eq. (48), we see that the condition (62) is verified for any value of Γ (with a decreasing factor that decays exponentially in N). Notice that the inequality $\lim_{N\to\infty} \tau^{(P)} \geqslant \lim_{N\to\infty} \tau^{(Q)}$ holds for any β, so that we have also $\lim_{\beta\to\infty} \lim_{N\to\infty} \tau^{(P)} \geqslant \lim_{\beta\to\infty} \lim_{N\to\infty} \tau^{(Q)}$. However, $\lim_{N\to\infty} \lim_{\beta\to\infty} \tau^{(Q)} = 2 \lim_{N\to\infty} \lim_{\beta\to\infty} \tau^{(P)}$, since, in general, $\lim_{\beta\to\infty} \tau^{(Q)} = 2 \lim_{\beta\to\infty} \tau^{(P)}$ [7].

G. Dissipation and decoherence at the critical point at zero temperature

The critical point at vanishing temperatures is intriguing. Indeed, if we choose N even and $j = N/2$, this setup coincides with the one used to investigate the quantum adiabatic algorithm [13]. From Eq. (44), for N large enough we have $\Gamma_c = \pm j$ and the GS is $m_z^{(1)} = \text{sgn}(\Gamma)j$. By using Eq. (57), from Eqs. (51) we see that, for any finite N, in the limit $\beta \to \infty$ the matrix A becomes triangular and, as a consequence, from Eq. (50) for its lowest nonzero eigenvalue μ_2 we obtain

$$\lim_{\beta\to\infty} \mu_2(A) = 2\gamma(2j - 1)\Delta^3, \quad (63)$$

where Δ is given by Eq. (44) evaluated at $|\Gamma| \leqslant |\Gamma_c| = j$. For N large enough, we thus have

$$\lim_{\beta\to\infty} \tau^{(P)} = \frac{N^2}{2\gamma\mathcal{J}^3}. \quad (64)$$

Moreover, for the property $\lim_{\beta\to\infty} \tau^{(Q)} = 2\lim_{\beta\to\infty} \tau^{(P)}$, we have also

$$\lim_{\beta\to\infty} \tau^{(Q)} = \frac{N^2}{\gamma\mathcal{J}^3}, \quad (65)$$

and therefore

$$\lim_{\beta\to\infty} \tau = \frac{N^2}{\gamma\mathcal{J}^3}. \quad (66)$$

The present thermalization time τ, which grows as N^2, is to be compared with the characteristic time to perform the quantum adiabatic algorithm [8], which grows as $\tau_{ad} \sim N/\Delta^2 = O(N^3)$. This difference must be attributed to the spontaneous emission process, the only mechanism at $T = 0$ by which the system, when in contact with the blackbody radiation, delivers its energy to the environment. Apparently, this mechanism provides a convergence toward the GS more efficient than that obtained in a slow transformation of the Hamiltonian parameters without dissipative effects.

VIII. NUMERICAL ANALYSIS OF ISOTROPIC LMG MODELS

We made an exact numerical analysis of Eq. (53) and of the eigenvalues of the matrix A provided by Eqs. (50) and (51). The numerical analysis confirms our analytical formulas and, besides, makes evident the existence of finite-size effects, which are a fingerprint of the phase transition.

Figure 1 provides 3D plots of $\tau_{m,n}$, as a function of m and n, calculated for a few choices of Γ and β. In agreement with Eqs. (55), the maximum of $\tau_{m,n}$ occurs in correspondence with $m \simeq n \simeq j/2$.

Figure 2 shows the behavior of $\tau_{m=j,n=j-1}$ (i.e., one of the components of the decoherence times $\tau_{m,n}$ close to $\tau^{(Q)} = \max_{m\neq n} \tau_{m,n}$) as a function of the system size N at different temperatures and for several values of Γ approaching the critical point Γ_c in both the paramagnetic and ferromagnetic regions. These plots confirm, in particular, that for β finite, $\tau_{m=j,n=j-1}$ diverges only at the critical point. More precisely, the divergence is linear in N for β sufficiently small, i.e., for $\beta \sim O(1/\Gamma) \sim O(1/\mathcal{J})$, in agreement with Eq. (60). A different situation occurs instead for $\beta \to \infty$, where the
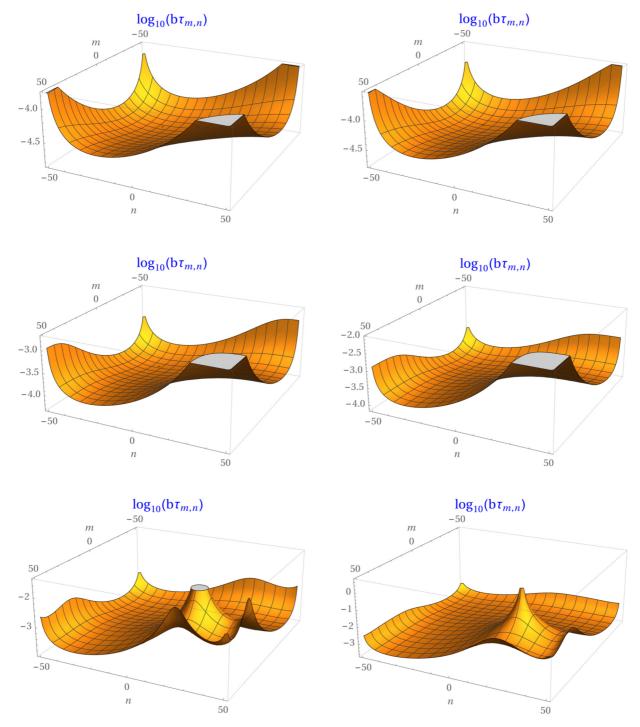
FIG. 1. Log plots of the dimensionless quantities $b\tau_{m,n}$, where $b = 2\gamma\mathcal{J}^3$, as a function of m and n, with $m \neq n$, obtained from Eq. (53) with $N = 100$, $j = N/2$, and, from top to bottom, $\Gamma = 2\Gamma_c$ (paramagnetic), $\Gamma = \Gamma_c$ (critical point), and $\Gamma = 0.5\Gamma_c$ (ferromagnetic), each evaluated at the dimensionless inverse temperatures $\beta\mathcal{J} = 1$ (left) and $\beta\mathcal{J} = 10$ (right). Notice that the left and right panels are different in each case.

divergence is quadratic in N and takes place for any Γ in the ferromagnetic region, in agreement with Eq. (65). Figure 2 also provides clear evidence of finite-size effects in proximity to the critical point, which are particularly important in the ferromagnetic region and at low temperatures. At some threshold $N_s(\beta,\Gamma)$, these finite-size effects decay approximately as power laws in N (notice that Fig. 2 is in log-log scale). In general, $N_s(\beta,\Gamma)$ turns out to be a

nongrowing function of β, whereas, for a given β, it grows for Γ approaching Γ_c.

Figure 3 shows $\tau^{(P)}$ as a function of the system size N. Unlike $\tau^{(Q)}$, we see that, whereas in the paramagnetic region, $\Gamma > \Gamma_c$, $\tau^{(P)}$ decays as a power law, in the ferromagnetic region, $\Gamma < \Gamma_c$, $\tau^{(P)}$ grows approximately as a power law even for β finite. Actually, the behavior of $\tau^{(P)}$ in the ferromagnetic region is not as smooth as shown in Fig. 3: by varying N
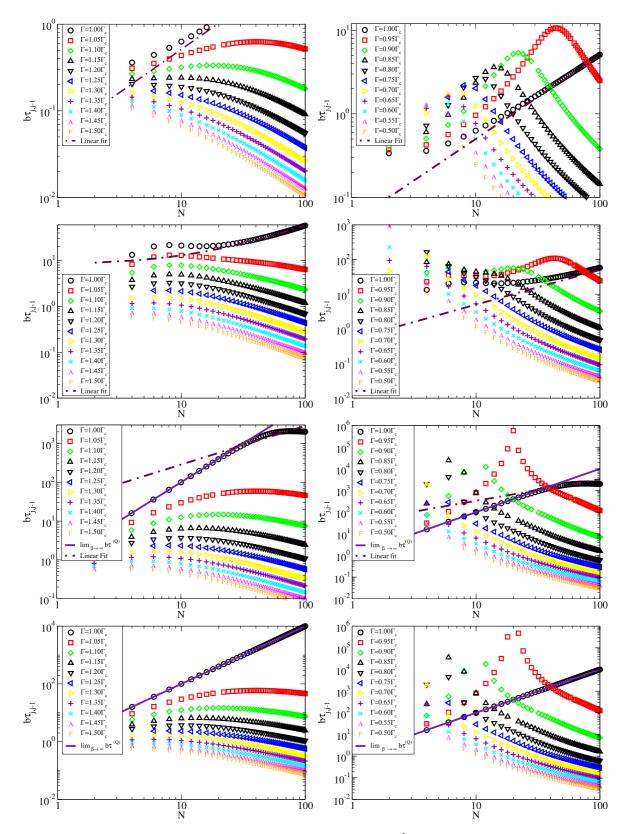
FIG. 2. Log-log plots of the dimensionless quantities $b\tau_{m=j,n=j-1}$, where $b = 2\gamma\mathcal{J}^3$, obtained from Eq. (53), as a function of N even, calculated for $j = N/2$, and several values of $\Gamma > 0$ approaching $\Gamma_c > 0$, Eq. (46), from above, i.e., in the paramagnetic region (left panels), and from below, i.e., in the ferromagnetic region (right panels). Different dimensionless inverse temperatures are considered, from top to bottom: $\beta\mathcal{J} = 1$, $\beta\mathcal{J} = 10$, $\beta\mathcal{J} = 100$, and $\beta\mathcal{J} = 1000$. The function $\lim_{\beta\to\infty}\tau^{(Q)}$ is obtained from Eq. (65). Notice however that, by definition, $\tau^{(Q)} = \max_{m\neq n}\tau_{m,n} \geq \tau_{j,j-1}$ (compare Fig. 1).
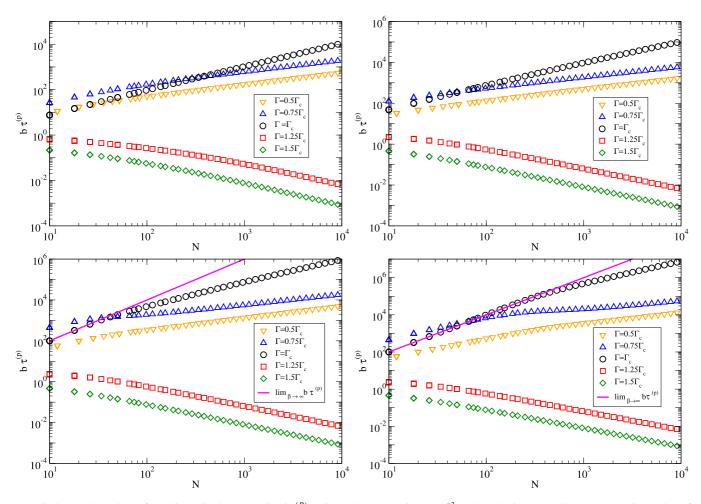
FIG. 3. Log-log plots of the dimensionless quantity $b\tau^{(P)} = b/\mu_2(\boldsymbol{A})$, where $b = 2\gamma\mathcal{J}^3$ and $\mu_2(\boldsymbol{A})$ is the smallest nonzero eigenvalue of $\boldsymbol{A}$, the matrix given by Eqs. (50) and (51), as a function of N even, evaluated for $j = N/2$ and several values of β and Γ, above and below the critical point Γ_c. Top left panel $\beta\mathcal{J} = 1$; top right panel $\beta\mathcal{J} = 10$; bottom left panel $\beta\mathcal{J} = 100$; bottom right panel $\beta\mathcal{J} = 1000$. The function $\lim_{\beta\to\infty}\tau^{(P)}$ is given by Eq. (64) evaluated at $0 < \Gamma \leqslant \Gamma_c$ (it provides the same limit in all the ferromagnetic region). For the present values of β, $\lim_{\beta\to\infty}\tau^{(P)}$ matches well with the data corresponding to $\Gamma = \Gamma_c$ and $\beta\mathcal{J} = 1000$ when $N \leqslant 10^3$. For larger values of β the agreement extends to greater values of N and also to data obtained for $\Gamma < \Gamma_c$.

we have periodic oscillations among three smooth curves associated with different sequences of N even. The data shown in Fig. 3 correspond to one of these sequences; for the other ones we have a power-law growth with a similar exponent but with a different prefactor.

Another fingerprint of the phase transition that takes place in the LMG model can be seen in Fig. 3 observing the agreement between Eq. (64) and $\tau^{(P)}$ when the latter is evaluated at larger and larger values of β (see bottom panels). More precisely, it turns that, for N sufficiently large, $\tau^{(P)}(\Gamma_c) \geqslant \tau^{(P)}(\Gamma)$ for any Γ, and that, for β sufficiently small, i.e., $\beta \sim O(1/\Gamma) \sim O(1/\mathcal{J})$, $\tau^{(P)}$ grows no more than linearly with N, while it grows no more than quadratically in N for β large.

IX. CONCLUSIONS

We have addressed the thermalization of the LMG model in contact with blackbody radiation. The analysis is done within LBA, a general mathematical setup developed in [7] which allows us to analyze the thermalization processes of extensive many-body systems. When applied to the LMG

model embedded in blackbody radiation, the LBA equations (which, in the fully coherent regime, coincide with the QOME) are relatively simple and can be studied analytically in great detail. A series of results emerge.

First, by analyzing the involved dipole-matrix elements, we find that, according to the conditions (11) and (14), in the general LMG model, i.e., independently of the anisotropy parameter γ_y, a full thermalization can take place only if the density is sufficiently high, while, in the limit of low density, the system thermalizes partially, namely, within the Hilbert subspaces $\mathcal{H}_j$ where the total spin has a fixed value.

Second, in the fully coherent regime, and for the isotropic case $\gamma_y = 1$, we are able to perform a comprehensive analysis of the thermalization. We evaluate the characteristic thermalization time τ almost analytically, as a function of the Hamiltonian parameters and of the system size N.

Third, we show that, as a function of N, τ diverges only at the critical point and in the ferromagnetic region. This divergence is no more than linear in N for β small, and no more than quadratic in N for β large. In particular, in the ferromagnetic region and at zero temperature, we prove that

τ diverges just quadratically with N, while quantum adiabatic algorithms lead to an adiabatic time that diverges with the cube of N.

The latter result sheds light on the problem of preparing a quantum system in a target state. If the target state is the GS of a subspace of the Hilbert space of the system, cooling the system at sufficiently small temperatures and ensuring, at the same time, that the system remains sufficiently confined in the chosen subspace, may produce an arbitrarily accurate result.

This procedure, at least for the present LMG model coupled to blackbody radiation, outperforms the procedure suggested by quantum adiabatic algorithms, where counterproductive costly efforts are spent to avoid dissipative effects. For more general many-body systems, it could be appropriate to consider cooling processes induced by different, possibly engineered, thermal reservoirs. The no-go theorem for exact ground-state cooling [42], which apparently prohibits the application of this idea, can be effectively evaded as discussed in [43].

[1] H.-P. Breuer and F. Petruccione, *The Theory of Open Quantum Systems* (Oxford University Press, New York, 2002).

[2] U. Weiss, *Quantum Dissipative Systems*, 3rd edition, Series in Modern Condensed Matter Physics, Vol. 13 (World Scientific, Singapore, 2008).

[3] G. Schaller, *Open Quantum Systems Far from Equilibrium* (Springer, Heidelberg, 2014).

[4] H. J. Lipkin, N. Meshkov, and A. J. Glick, Validity of many-body approximation methods for a solvable model. I. Exact solutions and perturbation theory, Nucl. Phys. **62**, 188 (1965).

[5] V. Gorini and A. Kossakowski, N-level system in contact with a singular reservoir, J. Math. Phys. **17**, 1298 (1976).

[6] M. Ostilli and C. Presilla, Toward a phenomenological theory of thermalization for quantum many-body systems: A Lindblad-based approach, arXiv:1611.03127.

[7] M. Ostilli and C. Presilla, Thermalization times of quantum many-body systems: A Lindblad-based approach (unpublished).

[8] V. Bapst, L. Foini, F. Krzakala, G. Semerjian, and F. Zamponi, The quantum adiabatic algorithm applied to random optimization problems: The quantum spin glass perspective, Phys. Rep. **523**, 127 (2013).

[9] R. Botet and R. Jullien, Large-size critical behavior of infinitely coordinated systems, Phys. Rev. B **28**, 3955 (1983).

[10] P. Ribeiro, J. Vidal, and R. Mosseri, Exact spectrum of the Lipkin-Meshkov-Glick model in the thermodynamic limit and finite-size corrections, Phys. Rev. E **78**, 021106 (2008).

[11] A. Das, K. Sengupta, D. Sen, and B. K. Chakrabarti, Infinite-range Ising ferromagnet in a time-dependent transverse magnetic field: Quench and ac dynamics near the quantum critical point, Phys. Rev. B **74**, 144423 (2006).

[12] S. Campbell, Criticality revealed through quench dynamics in the Lipkin-Meshkov-Glick model, Phys. Rev. B **94**, 184403 (2016).

[13] T. Caneva, R. Fazio, and G. E. Santoro, Adiabatic quantum dynamics of the Lipkin-Meshkov-Glick model, Phys. Rev. B **78**, 104426 (2008).

[14] T. Mori, Classical ergodicity and quantum eigenstate thermalization: Analysis in fully connected Ising ferromagnets, arXiv:1609.09258.

[15] S. Paganelli, F. de Pasquale, and S. M. Giampaolo, Decoherence slowing down in a symmetry-broken environment, Phys. Rev. A **66**, 052317 (2002).

[16] M. Lucamarini, S. Paganelli, and S. Mancini, Two-qubit entanglement dynamics in a symmetry-broken environment, Phys. Rev. A **69**, 062308 (2004).

[17] Y. Hamdouni and F. Petruccione, Time evolution and decoherence of a spin-1/2 particle coupled to a spin bath in thermal equilibrium, Phys. Rev. B **76**, 174306 (2007).

[18] H. T. Quan, Z. D. Wang, and C. P. Sun, Quantum critical dynamics of a qubit coupled to an isotropic Lipkin-Meshkov-Glick bath, Phys. Rev. A **76**, 012104 (2007).

[19] W. P. Wolf, The Ising model and real magnetic materials, Brazilian J. Phys. **30**, 794 (2000).

[20] A. Abragam and B. Bleaney, *Electron Paramagnetic Resonance of Transition Ions* (Oxford University Press, New York, 1970).

[21] J. R. Friedman, M. P. Sarachik, J. Tejada, and R. Ziolo, Macroscopic Measurement of Resonant Magnetization Tunneling in High-Spin Molecules, Phys. Rev. Lett. **76**, 3830 (1996).

[22] D. Porras and J. I. Cirac, Effective Quantum Spin Systems with Trapped Ions, Phys. Rev. Lett. **92**, 207901 (2004).

[23] J. I. Cirac, M. Lewenstein, K. Mølmer, and P. Zoller, Quantum superposition states of Bose-Einstein condensates, Phys. Rev. A **57**, 1208 (1998).

[24] T. Monz, P. Schindler, J. T. Barreiro, M. Chwalla, D. Nigg, W. A. Coish, M. Harlander, W. Hänsel, M. Hennrich, and R. Blatt, 14-Qubit Entanglement: Creation and Coherence, Phys. Rev. Lett. **106**, 130506 (2011).

[25] J. G. Bohnet, B. C. Sawyer, J. W. Britton, M. L. Wall, A. M. Rey, M. Foss-Feig, and J. J. Bollinger, Quantum spin dynamics and entanglement generation with hundreds of trapped ions, Science **352**, 1297 (2016).

[26] C. Gross, T. Zibold, E. Nicklas, J. Esteve, and M. K. Oberthaler, Nonlinear atom interferometer surpasses classical precision limit, Nature (London) **464**, 1165 (2010).

[27] M. F. Riedel, P. Bhi, Y. Li, T. W. Hänsch, A. Sinatra, and P. Treutlein, Atom-chip-based generation of entanglement for quantum metrology, Nature (London) **464**, 1170 (2010).

[28] I. D. Leroux, M. H. Schleier-Smith, and V. Vuletic, Implementation of Cavity Squeezing of a Collective Atomic Spin, Phys. Rev. Lett. **104**, 073602 (2010).

[29] Yong-Chang Zhang, Xiang-Fa Zhou, Xingxiang Zhou, Guang-Can Guo, and Zheng-Wei Zhou, Cavity-Assisted Single-Mode and Two-Mode Spin-Squeezed States via Phase-Locked Atom-Photon Coupling, Phys. Rev. Lett. **118**, 083604 (2017).

[30] N. Henkel, R. Nath, and T. Pohl, Three-Dimensional Roton-Excitations and Supersolid Formation in Rydberg-Excited Bose-Einstein Condensates, Phys. Rev. Lett. **104**, 195302 (2010).

[31] T. Macrì and T. Pohl, Rydberg dressing of atoms in optical lattices, Phys. Rev. A **89**, 011402 (2014).

[32] Y.-Y. Jau, A. M. Hankin, T. Keating, I. H. Deutsch, and G. W. Biedermann, Entangling atomic spins with a Rydberg-dressed spin-flip blockade, Nat. Phys. **12**, 71 (2016).

[33] J. Zeiher *et al.*, Many-body interferometry of a Rydberg-dressed spin lattice, Nat. Phys. **12**, 1095 (2016).

[34] M. Kitagawa and M. Ueda, Squeezed spin states, Phys. Rev. A **47**, 5138 (1993).

[35] L. I. R. Gil, R. Mukherjee, E. M. Bridge, M. P. A. Jones, and T. Pohl, Spin Squeezing in a Rydberg Lattice Clock, Phys. Rev. Lett. **112**, 103601 (2014).

[36] T. Macrì, A. Smerzi, and L. Pezzè, Loschmidt echo for quantum metrology, Phys. Rev. A **94**, 010102(R) (2016).

[37] A. W. Glaetzle, M. Dalmonte, R. Nath, C. Gross, I. Bloch, and P. Zoller, Designing Frustrated Quantum Magnets with Laser-Dressed Rydberg Atoms, Phys. Rev. Lett. **114**, 173002 (2015).

[38] R. M. W. van Bijnen and T. Pohl, Quantum Magnetism and Topological Ordering via Rydberg Dressing near Förster Resonances, Phys. Rev. Lett. **114**, 243002 (2015).

[39] T. Lahaye, C. Menotti, L. Santos, M. Lewenstein, and T. Pfau, The physics of dipolar bosonic quantum gases, Rep. Prog. Phys. **72**, 126401 (2009).

[40] M. Ostilli and C. Presilla, Fermi's golden rule for *N*-body systems in a blackbody radiation, Phys. Rev. A **94**, 032514 (2016).

[41] A. S. Davydov, *Quantum Mechanics* (Pergamon Press, London, Edinburgh, 1965).

[42] L.-A. Wu, D. Segal, and P. Brumer, No-go theorem for ground state cooling given initial system-thermal bath factorization, Sci. Rep. **3**, 1824 (2013).

[43] F. Ticozzi and L. Viola, Quantum resources for purification and cooling: Fundamental limits and opportunities, Sci. Rep. **4**, 5192 (2014).